Published by :
http://www.ijert.org

International Journal of Engineering Research & Technology (IJERT)
ISSN: 2278-0181
Vol. 8 Issue 09, September-2019

Influence of Surfactant Concentrations on N-Type Nanostructured Thermoelectric Oxide $CaMnO_{3-\delta}$

S. Berbeth Mary
Research Scholar, Department of Physics
St. Joseph's College (Autonomous)
Tiruchirappalli- 620 002
Tamil Nadu, India.

A. Leo Rajesh*
Assistant Professor, Department of Physics
St. Joseph's College (Autonomous),
Tiruchirappalli- 620 002,
Tamil Nadu, India.

***Abstract*:- Nano crystalline calcium manganite nanoparticles are promising n-type thermoelectric oxides at higher temperatures with perovskite orthorhombic structure have been synthesized by sol-gel hydrothermal method and the influence of surfactant polyvinyl pyrrolidone (PVP) concentration on $CaMnO_{3-\delta}$ nanoparticles were investigated. Systematic studies revealed that the surfactant concentration induces the average particle size of the nanoparticles. The synthesized nanoparticles were characterized by X-ray diffraction, scanning electron microscope with energy dispersive X-ray analysis and thermoelectric studies were done on the sintered sample between room temperature and 600 °C. Pure and crystalline $CaMnO_{3-\delta}$ nanoparticles were observed and the average particle size was calculated by Scherrer formula. Vibrational bands between 550-650 cm^{-1} confirms the formation of crystalline $CaMnO_{3-\delta}$ nanoparticle by FTIR analysis and peak intensity increases with increasing the concentration of PVP. Thermoelectric properties have been obtained for the pure, single phase sample with less average particle size without agglomeration and secondary phase. Optical studies revealed that $CaMnO_{3-\delta}$ nanoparticles having the absorption in the visible region and the indirect band gap was in the range of 2.14 eV- 2.41 eV using UV-Vis spectroscopy and the thermoelectric analysis showed the negative value of Seebeck coefficient of -287 μVK^{-1} at room temperature.**

Key words: Calcium manganite; PVP; sol-gel hydrothermal; electrical resistivity; thermopower.

1. INTRODUCTION

Thermoelectric energy system overcomes the limitations of energy resources and environmental pollution problems by converting the waste heat energy directly into electricity from industrial processes without any greenhouse gas emissions via the Seebeck effect, Peltier effect and vice versa. The energy conversion efficiency is estimated by the dimensionless figure of merit ZT [1]. The state of art alloys such as Bi_2Te_3, $CoSb_3$ are not chemically and thermally stable at higher temperatures under air atmosphere, but the discovery of $Na_xCoO_{2+\delta}$ by Terasaki et al. in 1997 initiated more research on oxides. Electron doped calcium manganite $Ca_{1-x}R_xMnO_3$ is extensively studied n-type thermoelectric oxide material because of its high electrical conductivity, oxidation resistant, and stability at elevated temperature. However, the undoped $CaMnO_{3-\delta}$ material has low carrier mobility due to ionic bonding which in turn reduces the thermopower of the material [2]. Materials with high electrical conductivity and Seebeck coefficient, together with a low thermal conductivity are potential candidates for thermoelectric devices. In bulk materials Seebeck coefficient, electrical conductivity and thermal conductivity are linked together by the electronic structure and they cannot be optimized independently, but band structure and phonon scattering can be engineered by nanostructured systems. Thermal conductivity can be reduced by producing the nanostructures with one or more dimensions smaller than the mean free path of phonons, but larger than that of the electrons without affecting the electrical conductivity. Nanostructuring can effectively enhance the ZT values by suppressing the thermal transport of phonons [3-5].

The product obtained from sol-gel method is amorphous in nature while the yield is very less in hydrothermal method. Sol-gel hydrothermal method is a suitable method for synthesizing the thermoelectric metal oxide nanoparticles due to controlled grain size, morphology, high surface area for large scale application. The parameters such as pH, precursor, addition of surfactants, experimental temperature and duration induces the growth mechanism of the nanoparticles. The expected nanostructures within the range can be achieved by the systematic studies on these parameters [6, 7]. Annealing in air atmosphere at higher temperatures leads to the formation of perovskite oxides, but it affects the growth mechanism, homogeneity, surface area [8].

A surfactant is essential in wet chemical metal oxide synthesis process to form discrete nanoparticles than network and it controls the grain growth by regulating the reaction kinetics. Surfactants are used in aqueous synthesis to reduce the interfacial energy and hence control the growth mechanism in nanoparticles. Particle agglomeration is being avoided by forming an absorption layer by a surfactant on the surface of the nanoparticle and regulates the grain growth of the particle. In metal oxide nanoparticle synthesis process, surfactants are acting as chelating agent, capping agent, template and fuels. Citric acid as a chelating agent modifies the synthesis process and the formation of perovskite oxide occurs at lower annealing temperature [9-12].

Reducing the annealing temperature and duration decreases the size of the nanoparticles that leads to the low thermal conductivity which in turn improves the thermopower [13, 14]. Non-toxic and non-ionic polymer Polyvinyl pyrrolidone (PVP) with the functional groups C=O, C-N, CH_2

International Journal of Engineering Research & Technology (IJERT)
ISSN: 2278-0181
Vol. 8 Issue 09, September-2019

is used in synthesizing nanoparticles [15, 16]. PVP as a capping agent initially increases the particle size by forming an absorption layer on the nanoparticle, and then particle size reduces during annealing by burning the PVP polymer [17-19]. The reduction of grain size by nanostructuring and addition of surfactants induces the phonon scattering; as a result the lattice thermal conductivity reduces which will then improves the thermopower of the material [20, 21].

In this research paper, n-type thermoelectric oxide $CaMnO_{3-\delta}$ nanoparticles have been synthesized by sol-gel hydrothermal method and the role of surfactants as chelating and capping agent are investigated. The influence of polyvinyl pyrrolidone on structural, morphological, electrical and thermoelectric properties has been optimized based on the size, crystallinity and surface morphology of the nanoparticles for the application of thermoelectrics.

2. EXPERIMENTAL PROCEDURE

2.1. Preparation of $CaMnO_{3-\delta}$ nanoparticles

AR grade calcium nitrate tetrahydrate (≥99%), manganese nitrate hydrate (≥98%), and ammonium hydroxide solution were used as precursors without further purification. Citric acid and polyvinyl pyrrolidone (PVP, MW≈40000 g/m) are used as chelating and capping agent respectively. Stoichiometric amounts of metal nitrates of Ca $(NO_3)_2$. $4H_20$, $Mn(NO_3)_2$. H_2O were weighed at 1:1 molar ratio and dissolved in distilled water. Citric acid solution was added to the mixture in the mole ratios 1:1 (citric acid: metal ion) and PVP solution was added to the precursor solution with different concentrations of 1g, 2g, and 3g. Homogeneous solution was obtained after stirring for 30 minutes and ammonium hydroxide was added drop wise till its pH reaches 9.2, then it heated at 80 °C till it reduced to the half of the amount of it. Then this sol was transferred into a Teflon lined stainless steel autoclave, which is placed it in hot air oven at 200 °C for 20 hours. The product was cleaned with distilled water and ethanol to remove the organic substances, then dried and annealed at 950 °C to attain $CaMnO_{3-\delta}$ nanopartices.

2.2. Characterization Techniques

Structural characterization of the $CaMnO_{3-\delta}$ samples were carried out by using Bruker D8 advance diffractometer equipped with Cu Kα radiation (λ = 1.5406 Å) with 2θ ranging between 10° and 80° with a step size of 0.02°. The surface morphology of the samples were analyzed using a JEOL JSM 5600 scanning electron microscope and its elemental analysis was accomplished by Energy Dispersive X-ray analysis (EDAX). Perklin Elmer Fourier Transform Infrared Spectrometer is used to capture the FTIR spectrum of the samples. Optical characterization was done by Bruker Lambda 35 UV- Visible spectrometer and Tauc's relation used to calculate the band gap value. The annealed powders were compacted with 3 wt % of paraffin wax as a binder at 50Mpa and sintered at 850°C with a heating rate of 10°C/min for 4 h by the conventional sintering process for thermoelectric measurement. LSR-3, Seebeck, Linseis, Germany, investigated thermoelectric properties such as Seebeck coefficient (S), electrical conductivity (σ) and the power factor ($S^2\sigma$) of surfactant assisted $CaMnO_{3-\delta}$ nanoparticles were investigated between ambient and 600°C with ΔT=50°C with highly pure helium atmosphere.

3. RESULTS AND DISCUSSION

3.1. Structural analysis of $CaMnO_{3-\delta}$ nanoparticles

XRD measurement was used to find the purity and crystallinity and influence of PVP on $CaMnO_{3-\delta}$ nanoparticles. Figure 1(a-d) represents the powder XRD pattern of the pure $CaMnO_{3-\delta}$ nanoparticles with different concentrations of PVP 0g, 1g, 2g, and 3g. All the diffraction patterns were indexed and matched with the JCPDS card No: 461009. Orthorhombic $CaMnO_{3-\delta}$ with the space group of Pbam were identified with the lattice parameters a=5.424 Å, b= 10.23 Å, c= 3.735 Å and unit cell volume V= 207.25 $Å^3$ [22]. Peaks at 2θ = 19.00º, and 31.26º are observed as minor phases of Co_3O_4 (JCPDS card no: 431003) along with the peaks of $CaMnO_{3-\delta}$ nanoparticles. As surfactant concentration increases, the intermediate phase Co_3O_4 gradually disappears and hence the remaining peaks are attributed to $CaMnO_{3-\delta}$ nanoparticles. When the surfactant exceeds the limit of saturation i.e, 3g then there was a secondary peak of PVP at 2θ = 20.23º and this could be seen while synthesizing the nanoparticles as precipitation which is good agreement with the reported data [23]. The addition of PVP as a capping agent improves the crystallinity and reduces the average crystallite size of the sample, indicating that this surfactant plays an important role in synthesizing nanoparticles.

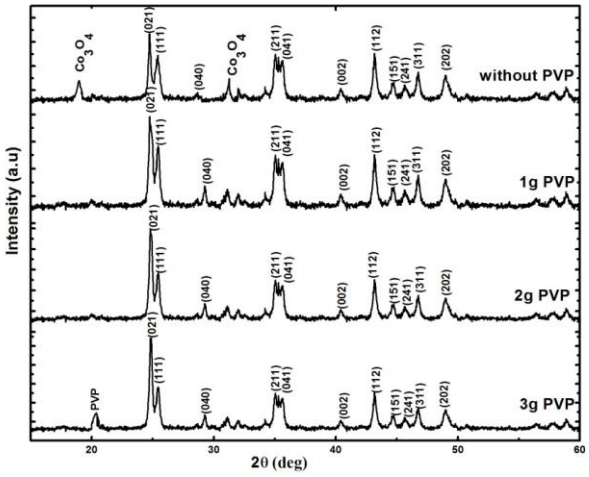

Figure 1. XRD pattern of $CaMnO_{3-\delta}$ nanoparticles (a) without PVP (b) with 1g PVP (c) with 2g PVP (d) with 3g PVP

The average crystallite size was estimated by Scherrer formula and it is denoted as D= Kλ/ βcosθ, where K, λ, β, θ are the Scherrer constant (K=0.9), the wavelength of the radiation Cu Kα (λ = 1.5406 Å), full width at half maximum of the diffraction peaks, and the Bragg's angle respectively. The size of the nanoparticles decreases with increasing the concentration of PVP and the calculated average particle size of $CaMnO_{3-\delta}$ nanoparticles with 3g, 2g, 1g of PVP, and without PVP is 11, 15, 42, and 71 nm respectively [24, 25].

3.2. Surface morphology and chemical composition of $CaMnO_{3-\delta}$ nanoparticles

Figure. 2 represents the surface morphology and EDAX spectrum of surfactant assisted $CaMnO_{3-\delta}$ nanoparticles

International Journal of Engineering Research & Technology (IJERT)
ISSN: 2278-0181
Vol. 8 Issue 09, September-2019

(a, b) without PVP, (c, d) 1g of PVP, (e, f) 2g of PVP, (g, h) 3g of PVP. SEM images shows that the samples have spherical shaped well defined nanoparticles without agglomeration for lower concentration of PVP. When the concentration of PVP exceeds the solubility limit then agglomerated particles are formed [26]. The capping agents form an absorption layer while synthesizing the nanoparticles and then the capped polymer disappear during annealing process and hence the average grain size reduces. The average grain size decreases with increasing the concentration of PVP, due to the burning of more mount of PVP polymer during annealing process.

Elemental composition confirmed the presence of elements with the cationic ratio 1:1 of Ca:Mn is shown in table 1. Oxygen deficient $CaMnO_{3-\delta}$ nanoparticles are observed for all the samples, indicating that the PVP molecules occupy the vacancy of oxygen. Consequently, we can infer that the synthesized $CaMnO_{3-\delta}$ nanoparticle is an oxygen deficient material which could be removed to improve the thermopower.

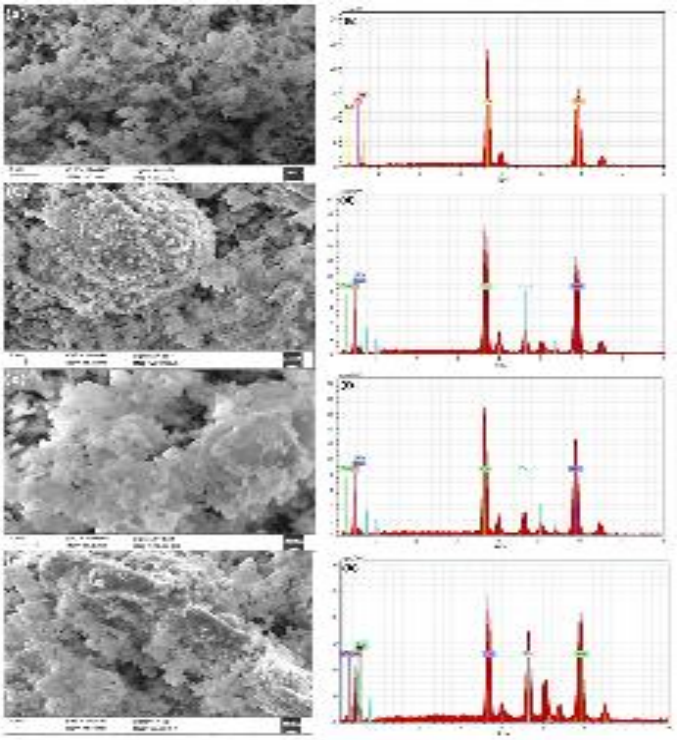

Figure 2. SEM and EDAX pattern of $CaMnO_{3-\delta}$ nanoparticles (a, b) without PVP (c, d) with 1g PVP (e, f) with 2g PVP (g, h) with 3g PVP

Table 1. Compositional values of the synthesized $CaMnO_{3-\delta}$ nanoparticles based on EDAX analysis

Sample	Element	Series	Atomic %	Ca/Mn
$CaMnO_{3-\delta}$ without PVP	Ca	K	24.43	1.03
	Mn	K	23.56	
	O	K	52.01	
$CaMnO_{3-\delta}$ with 1g of PVP	Ca	K	22.54	1.10
	Mn	K	20.42	
	O	K	57.04	
$CaMnO_{3-\delta}$ with 2g of PVP	Ca	K	21.42	1.05
	Mn	K	20.38	
	O	K	58.20	
$CaMnO_{3-\delta}$ with 3g of PVP	Ca	K	22.67	1.21
	Mn	K	18.81	
	O	K	58.52	

3.3. Functional group analysis of $CaMnO_{3-\delta}$ nanoparticles

The FTIR spectra of PVP assisted $CaMnO_{3-\delta}$ nanoparticles are shown in figure. 3. The OH-stretching and HOH- bending vibrational bands are observed at 3420 cm^{-1} and 1594 cm^{-1} are due to the physically adsorbed water molecule. The peak intensity increases with increasing the concentration of PVP, indicating that the presence of large amounts of carbon in the sample due to excess amount of PVP [27]. Average particle size influences the bands by a small shift which could be attributed to the addition of PVP as a capping agent [28]. Interaction between metal ions and PVP through oxygen C=O group of the polymer is the reason behind the shift in the bands [29]. The symmetric stretching occurs at 855 cm^{-1} indicates the vibration of NO_3 ions and the standard peak of $CaMnO_{3-\delta}$ was appeared in the region of 550- 650 cm^{-1} [30].

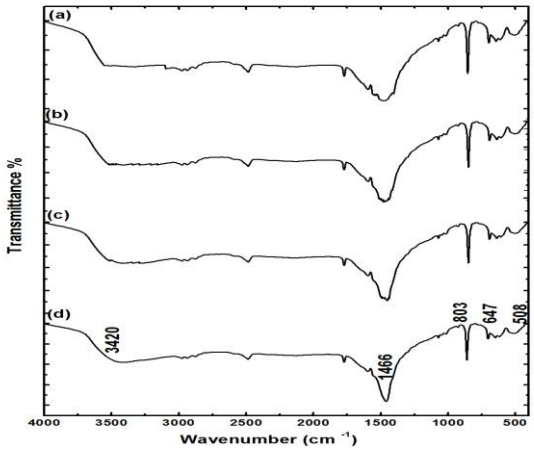

Figure 3. FTIR spectrum of $CaMnO_{3-\delta}$ nanoparticles (a) without PVP (b) with 1g PVP (c) with 2g PVP (d) with 3g PVP

3.4. Optical properties of $CaMnO_{3-\delta}$ nanoparticles

Figure. 4 (a) represents the absorbance spectra and (b) indirect energy band gap (E_g) of surfactant assisted $CaMnO_3$ nanoparticles by UV-Vis spectroscopy. Absorption spectra of the samples are recorded in the range of 200-800 nm and it is observed that the absorption spectra shows a wide range of absorption with a broad peak around 300 nm. As PVP concentration increases from 0g to 3g the band gap edges changes between 380 nm and 440 nm and then it sharply moved to lower wavelength regions, indicating that $CaMnO_{3-\delta}$ nanoparticle is an indirect band gap material. This absorption spectra shift to a lower wavelength due to the larger band gap of the nanoparticles.

The band gap E_g was calculated from the equation $(\alpha h\nu)^n = B(h\nu - E_g)$, Where α is the absorption coefficient, $h\nu$ is the photon energy, B is dimensional constant, and n is the index representing the transmission order, where n=2 for direct band gap and n=1/2 for an indirect band gap. The band gap was determined by extrapolating the linear portion of the plot relating $(\alpha h\nu)^{1/2}$ versus $h\nu$ (eV) is shown in figure 4 (b). The calculated band gap energies of $CaMnO_{3-\delta}$ nanoparticles at different PVP concentrations of 0g, 1g, 2g and 3g are 2.14 eV, 2.22 eV, 2.30 eV and 2.42 eV. The results indicate that the $CaMnO_3$ nanoparticle is an indirect, wide band gap semiconducting material. As the concentration of PVP increases, the crystallite size of the material decreases. As a result the band gap energy of the material increases. This

International Journal of Engineering Research & Technology (IJERT)
ISSN: 2278-0181
Vol. 8 Issue 09, September-2019

increased band gap due to decreased crystallite size is attributed to the quantum confinement effect of $CaMnO_{3-\delta}$ nanoparticles.

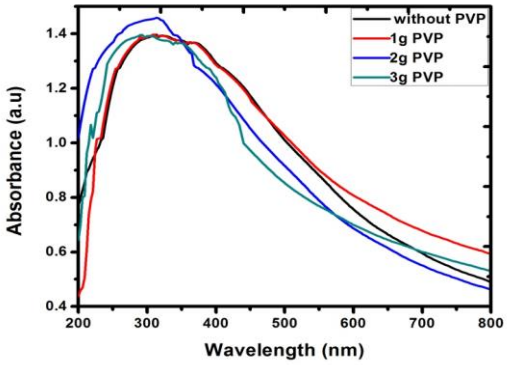

Figure 4 (a) Absorption spectra of $CaMnO_{3-\delta}$ nanoparticles (a) without PVP (b) with 1g PVP (c) with 2g PVP (d) with 3g PVP

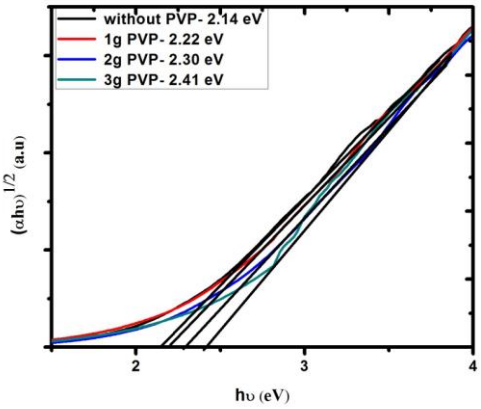

Figure 4 (b) Indirect Band gap of $CaMnO_{3-\delta}$ nanoparticles (a) without PVP (b) with 1g PVP (c) with 2g PVP (d) with 3g PVP

3.5. Thermoelectric property of $CaMnO_{3-\delta}$ nanoparticles

Figure. 5 depicts the temperature dependence of Seebeck coefficient S(T) and electrical resistivity of surfactant optimized $CaMnO_{3-\delta}$ nanoparticle annealed at 950 °C under air atmosphere with 2g of PVP, where the negative Seebeck coefficient value indicating that the sample is n- type material. The absolute Seebeck coefficient value and electrical resistivity at room temperature is -287 μV/K and 7.4 Ω cm.

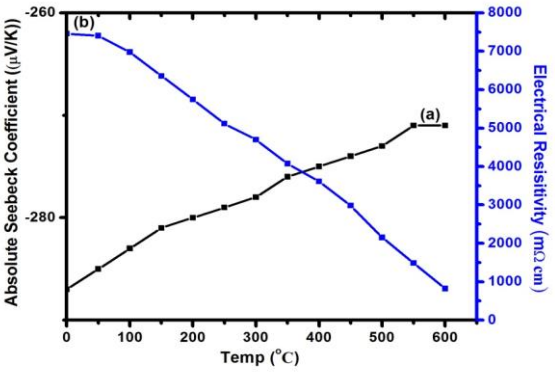

Figure 5. Absolute Seebeck coefficient and electrical resistivity of $CaMnO_{3-\delta}$ nanoparticles with 2g of PVP annealed at 950 °C under air atmosphere

Figure. 6 represents the power factor of the $CaMnO_{3-\delta}$ nanoparticles with 2g of PVP. According to Mott's adiabatic small polaron conduction model the transport properties can be described as $\rho = \rho_0 T \exp(E_a/ k_B T)$ where ρ, E_a, k_B are resistivity, activation energy and Boltzman's constant respectively. By using the Arrhenius plot of ln (σT) versus 1000/T and the linear fitting method is used to calculate the activation energy and it was found that 0.08 eV. Power factor increases with increasing temperature.

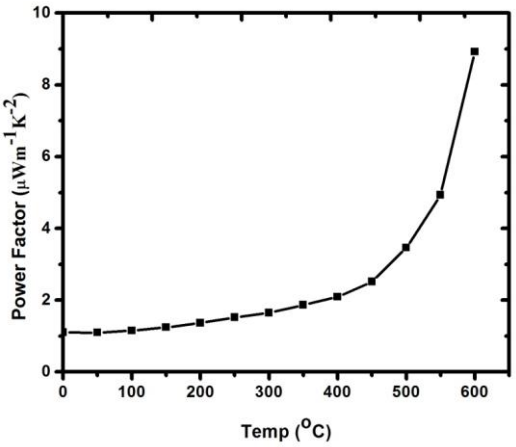

Figure 6. Power factor of $CaMnO_{3-\delta}$ nanoparticles with 2g of PVP annealed at 950 °C under air atmosphere

4. CONCLUSION

Orthorhombic perovskite structured $CaMnO_{3-\delta}$ nanoparticles were synthesized by sol-gel hydrothermal method at 200 °C, and the influence of PVP was studied. The average particle size increases with increasing the concentration of PVP, but higher PVP concentration yields the agglomerated nanoparticles with the secondary phase of PVP. FTIR analysis confirmed the formation of crystalline $CaMnO_{3-\delta}$ nanoparticle with the bands between 550 and 650 cm^{-1}. The Larger amount of carbon in the sample due to excess amount of PVP increased the peak intensity and the shift is due to the interaction between metal ions and PVP molecules. The absolute Seebeck coefficient, electrical resistivity, activation energy and the power factor are obtained for the PVP optimized $CaMnO_{3-\delta}$ nanoparticle. From the above results, $CaMnO_{3-\delta}$ nanoparticle with 2g of PVP is a suitable candidate for the fabrication of thermoelectric devices at higher temperature.

REFERENCES

[1] D.M. Rowe, Thermoelectrics, an environmentally-friendly source of electrical power, Renew. Ener., 16 (1-4) (1999) 1251–1256. Doi : 10.1016/S0960-1481(98)00512-6.

[2] Mohamed Mouyane, Brahim Itaali, Jérôme Bernard, David Houivet, Jacques G. Noudem, Flash combustion synthesis of electron doped-$CaMnO_3$ thermoelectric oxides, Powder Tech 264 (2014) 71–77. Doi: 10.1016/j.powtec.2014.05.022.

[3] G. J. Snyder, E. S. Toberer, Complex thermoelectric materials, Nat. Mater., 7(2) (2008) 105–114. Doi: 10.1038/nmat2090.

[4] R. Venkatasubramanian, E. Siivola, T. Colpitts B. Quinn, Nature., 413 (2001) 597–602. Doi: 10.1038/35098012.

[5] Majumdar A, Thermoelectricity in Semiconductor Nanostructures, Science., 303 (2004) 777–778. Doi: 10.1126/science.1093164.

[6] Jeroen Spooren Richard, I.Walton, Hydrothermal synthesis of the perovskite manganites $Pr_{0.5}Sr_{0.5}MnO_3$ and $Nd_{0.5}Sr_{0.5}MnO_3$ and alkali-earth manganese oxides $CaMn_2O_4$, 4H-$SrMnO_3$, and 2H-BaMnO3, Hydrothermal synthesis of the perovskite manganites $Pr_{0.5}Sr_{0.5}MnO_3$ and $Nd_{0.5}Sr_{0.5}MnO_3$ and alkali-earth manganese oxides $CaMn_2O_4$, 4H-$SrMnO_3$, and 2H-$BaMnO_3$, J. Solid State Chem., 178 (5) (2005) 1683-1691. Doi:10.1016/j.jssc.2005.03.006.

[7] Masahiro Yoshimura, Importance of soft processing of advanced materials for sustainable society, Procedia Engineering., 171 (2017) 40-52. Doi: 10.1016/j.proeng.2017.01.308.

[8] L.M. Fang, X.T. Zu, Z.J. Li, S. Zhu, C.M. Liu, W.L. Zhou, L.M. Wang, Synthesis and characteristics of Fe^{3+}-doped SnO_2 nanoparticles via sol–gel-annealing or sol–gel-hydrothermal route, J. Alloys Compd., 454 (2008) 261–267. Doi: 10.1016/j.jallcom.2006.12.014. 1

[9] Luminita Predoana, Andrei Jitianu, Silviu Preda, Barbara Malic & Maria Zaharescu, Thermal behavior of Li–Co-citric acid water-based gels as precursors for $LiCoO_2$ powders, J. Therm Anal Calorim (2015) 119:145-153. Doi: 10.1007/s10973-014-4178-4.

[10] F. Deganello, G. Marcì, G. Deganello, Citrate–nitrate auto-combustion synthesis of perovskite-type nanopowders: A systematic approach, J. Eur. Ceram. Soc., 29 (2009) 439–450. Doi: 10.1016/j.jeurceramsoc.2008.06.012.

[11] A. Mali, A. Ataie, Influence of the metal nitrates to citric acid molar ratio on the combustion process and phase constitution of barium hexaferrite particles prepared by sol–gel combustion method, Ceram. Int., 30 (2004) 1979–1983. Doi: 10.1016/j.ceramint.2003.12.178.

[12] M. Khazaei1, A. Malekzadeh, F. Amini, Y. Mortazavi, A. Khodadadi, Effect of citric acid concentration as emulsifier on perovskite phase formation of nano-sized $SrMnO_3$ and $SrCoO_3$samples, Cryst. Res. Technol. 45 (10) (2010) 1064 – 1068. Doi: 10.1002/crat.201000258.

[13] Mosleh, P. Kamelin , M. Ranjbar, H. Salamati, Effect of annealing temperature on structural and magnetic properties of Ba $Fe_{12}O_{19}$ hexaferrite nanoparticles, Ceram. Int., 40 (2014) 7279– 7284. Doi: 10.1016/j.ceramint.2013.12.068.

[14] Phan, C. M, Nguyen, H. M, Role of Capping Agent in Wet Synthesis of Nanoparticles, J. Phys.Chem. A., 121(17) (2017) 3213–3219. Doi:10.1021/acs.jpca.7b02186.

[15] S. V. Jadhav, D. S. Nikam, V. M. Khot, N. D. Thorat, M. R. Predator, R. S. Ningthoujam, A. B. Salunkhe, S. H. Pawar, Studies on colloidal stability of PVP-coated LSMO nanoparticles for magnetic fluid hyperthermia, New J. Chem.**,** 2013,37, 3121-3130. Doi: 10.1039/C3NJ00554B.

[16] Tie Liu, Jingyuan Liu, Qi Liu, Yanbo Sun, Xiaoyan Jing, Hongquan Zhang, Jun Wang, Three-dimensional hierarchical Co_3O_4nano/micro-architecture: synthesis and ethanol sensing properties. CrystEngComm**,** 2019. Doi: 10.1039/C9CE01086F.

[17] Tongfang Yin, Dawei Liu, Yun Ou, Feiyue Ma, Shuhong Xie, Jing-Feng Li, Jiangyu Li, Nanocrystalline Thermoelectric $Ca_3Co_4O_9$ Ceramics by Sol-Gel Based Electrospinning and Spark Plasma Sintering, J. Phys. Chem. C 2010, 114, 10061–10065. Do: 10.1021/jp1024872. Ch. Kanchana Lata, Mucherla Raghasudha, Y. Aparna, Mc. Ramchander, D. Ravinder, Ke.Jaipal, P. Veerasomaiah, D. Shridhar, Effect of Capping Agent on the Morphology, Size and Optical Properties of In_2O_3 Nanoparticles. Mat. Res., 20 (1) (2017) 256–263. Doi:10.1590/1980-5373-mr-2016-0292.

[18] R. Ma, K. Takada, K. Fukuda, N. Iyi, Y. Bando, T. Sasaki,Topochemical synthesis of monometallic (Co2+-Co3+) layered double hydroxide and its exfoliation into positively charged $Co(OH)_2$ nanosheets. Angew. Chem. Int. Ed. 47 (2008) 86–89. Doi : 10.1002/anie.200703941.

[19] J.W. Park, D.H. Kwak, S.H. Yoon, S.C. Choi, Thermoelectric properties of Bi, Nb co-substituted $CaMnO_3$ at high temperature, J. Alloys Compd., 487 (2009) 550–555. Doi: 10.1016/j.jallcom.2009.08.012.

[20] Ravindra K. Gupta, Eun Yi Kim, Yoo Hang Kim, Chin Myung Whang, Effect of strontium ion doping on structural, thermal, morphological and electrical properties of a co-doped lanthanum manganite system, J. Alloys Compd., 490 (2010) 56–61. Doi: 10.1016/j.jallcom.2009.10.095.

[21] Yang Wang, Yu Sui, Hongjin Fan, Xianjie Wang, Yantao Su, Wenhui Su, Xiaoyang Liu, High Temperature Thermoelectric response of Electron-Doped CaMnO3. Chem. Mater. 2009, 21, 4653–4660 4653. Doi:10.1021/cm901766y.

[22] Jing-Fang Zhu, Guo-Hong Tao, Hang-Yu Liu, Ling He, Qian-Hui Sun, Hai-Chao Liu, Aqueous-phase selective hydrogenation of phenol to cyclohexanone over soluble Pd nanoparticles. Green chem.., 02-07.Doi: 10.1039/c0xx00000x.

[23] B. D. Gulity, Elements of X-ray diffraction., 2nd ed, Addition –Wesley, USA,(1987).

[24] Marcela F. Silva, Luiz A. S. de Oliveira, Mariani A. Ciciliati, Michele K. Lima, Flávio F. Ivashita, Daniela M. Fernandes de Oliveira, Ana Adelina W. Hechenleitner, Edgardo A. G. Pineda, The Effects and Role of Polyvinylpyrrolidone on the Size and Phase Composition of Iron Oxide Nanoparticles Prepared by a Modified Sol-Gel Method. J. Nanomat., 2017. Doi: 10.1155/2017/7939727.

[25] Hang Sun, Jiating He, Jiangyan Wang, Shuang-Yuan Zhang, Cuicui Liu, Thirumany Sritharan, Subodh G Mhaisalkar, Ming-Yong Han, Dan Wang, and Hongyu Chen. Investigating the Multiple Roles of Polyvinylpyrrolidone for A General Methodology of Oxide Encapsulation. J. Am. Chem. Soc., (2013). Doi: 10.1021/ja4035335.

[26] Marijan Gotic, Svetozar Music, Mo¨ssbauer, FT-IR and FE SEM investigation of iron oxides precipitated from $FeSO_4$ solutions, J. Molecular Structure., 834–836 (2007) 445–453.Doi: 10.1016/j.molstruc.2006.10.059.

[27] Babu KS, Reddy AR, Reddy KV, Mallika AN. High thermal annealing effect on structural and optical properties of ZnO–SiO_2 nanocomposite. Mater Sci Semicond Process., 2014;27:643–8.

[28] KV Anasuya, MK Veeraiah, P Hemalatha, Synthesis and Characterization of Poly (Vinylpyrrolidone) -Copper (II) Complexes. Res.J.chem.sci., 5 (2) (2015) 64-69.

[29] F.P. Zhang, Q.M. Lu, X. Zhang, J.X. Zhang, First principle investigation of electronic structure of $CaMnO_3$ thermoelectric compound oxide, J. Alloy Compd., 509 (2011) 542–545. doi:10.1016/j.jallcom.2010.09.102.

[30] A. N. Mallika, A. Ramachandra Reddy, K. Venugopal Reddy. Annealing effects on the structural and optical properties of ZnO nanoparticles with PVA and CA as chelating agents. J. Advanced Cera., 2015, 4(2): 123-129. Doi: 10.1007/s40145- 015-0142-4.